Electronic Supplementary Information

Correlation between the electronic/local structure and CO-oxidation activity of Pd_xRu_{1-x} alloy nanoparticles

Chulho Song,[a] Akhil Tayal,[a] Okkyun Seo,[ba] Jaemyung Kim,[a] Yanna Chen,[ba] Satoshi Hiroi,[b] L. S. R. Kumara,[a] Kohei Kusada,[c] Hirokazu Kobayashi,[c] Hiroshi Kitagawa,[c] and Osami Sakata*[abd]

[a] *Synchrotron X-ray Station at SPring-8, Research Network and Facility Services Division, National Institute for Materials Science, 1-1-1 Kouto, Sayo, Hyogo 679-5148, Japan*

[b] *Synchrotron X-ray Group, Research Center for Advanced Measurement and Characterization, National Institute for Materials Science, 1-1-1 Kouto, Sayo, Hyogo 679-5148, Japan*

[c] *Division of Chemistry, Graduate School of Science, Kyoto University, Kitashirakawa Oiwake-cho, Sakyo-ku, Kyoto 606-8502, Japan*

[d] *Department of Innovative and Engineered Materials, Tokyo Institute of Technology, 4259-J3-16, Nagatsuta, Midori, Yokohama 226-8502, Japan*

*Corresponding author: SAKATA.Osami@nims.go.jp

SUPPORTING NOTE A. Particle size distributions of Pd_xRu_{1-x} nanoparticles (NPs)

Supplementary Figure 1 shows the particle size distribution of Pd_xRu_{1-x} NPs. The mean diameters of the All NPs were determined from the TEM images to be **a)** Ru (6.6 ± 1.4), b**)** $Pd_{0.1}Ru_{0.9}$ (9.4 ± 1.8), **c)** $Pd_{0.3}Ru_{0.7}$ (10.4 ± 1.9), **d)** $Pd_{0.5}Ru_{0.5}$ (10.7 ± 2.8), **e)** $Pd_{0.7}Ru_{0.3}$ (8.2 ± 1.6), **f)** $Pd_{0.9}Ru_{0.1}$ (8.6 ± 1.4), **g)** Pd (9.8 ± 2.6), respectively. Numbers that follow the ± sign represent estimated standard deviations.

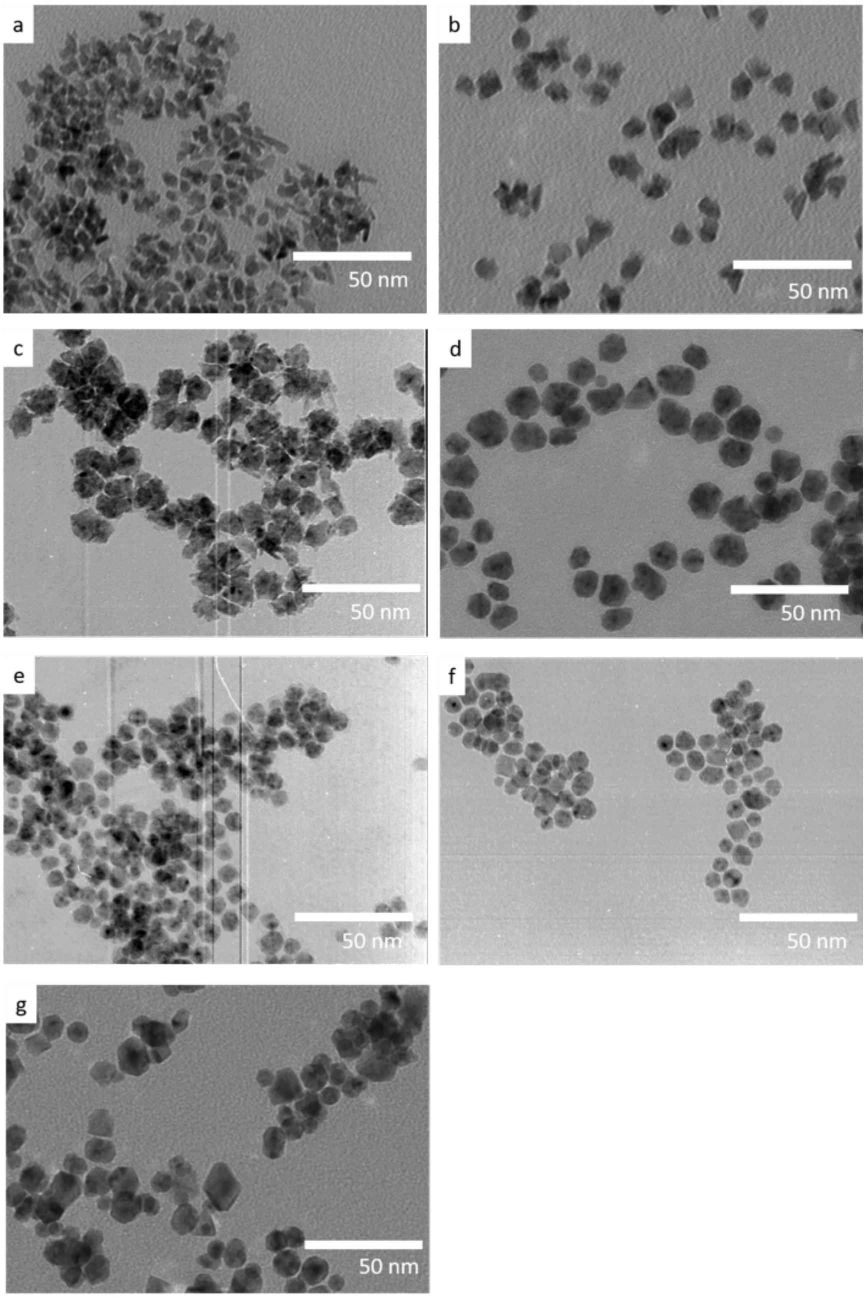

Figure S1. Particle size distributions of Pd_xRu_{1-x} NPs:

a, x = 0; **b**, x = 0.1; **c**, x = 0.3, **d**, x = 0.5; **e**, x = 0.7; **f**, x = 0.9, **g**, x = 1.0.

SUPPORTING NOTE B. Temperature for 50% conversion of CO to CO_2 (T_{50}) for Pd_xRu_{1-x} NPs

Catalyst Preparation

To investigate the CO oxidizing catalytic activities of Pd_xRu_{1-x} (x = 0, 0.1, 0.3, 0.5, 0.7, 0.9, 1.0) NPs supported on γ-Al_2O_3 catalysts were prepared by wet impregnation. Each NPs (equivalent to 1 wt % of γ-Al_2O_3) was ultrasonically dispersed in purified water. γ-Al_2O_3 support that had been pre-calcined at 1073 K for 5 h was put into each aqueous solution of nanoparticles, and then the suspended solutions were stirred for 12 h. After stirring, the suspended solutions were heated to 60 °C and dried under vacuum. The resulting powders were kept at 120 °C for 8 h to remove water completely.

Catalytic Tests

The obtained catalyst powders were pressed into pellets at 1.2 MPa for 5 min. The pellets were crushed and sieved to obtain grains with diameters between 180 and 250 μm. Each supported nanoparticle catalyst (150 mg) was loaded into a tubular quartz reactor (i.d. 7 mm) with quartz wool. CO/O_2/He mixed gas (He/CO/O2: 49/0.5/0.5 mL/min) was passed over the catalysts at ambient temperature, and the catalysts were then heated to 100 °C. After 15 min, effluent gas was collected, and the reaction products were analyzed by gas chromatography with a thermal conductivity detector (GC-8A, Shimadzu, Japan). Catalysts were heated in increments of 10 °C to a temperature at which CO was consumed completely, and the products were analyzed at each temperature.

SUPPORTING NOTE C. fitting results of EXAFS

The EXAFS fitting of all the samples was carried out using a single shell. For all the spectra measured at Ru K-edge the first shell is considered to be made up of Ru-Ru, and similarly, for the spectra measured at Pd *K*-edge Pd-Pd atomic pair was considered as the first shell. The value of passive electron reduction factor (S02) obtained from fitting the Ru reference, and Pd reference is 0.86 and 0.88, respectively. The value of S02 for all the spectra measured at Ru *K*-edge was fixed to 0.86. Similarly, the value of S02 for the spectra measured at Pd *K*-edge was set at 0.88. Due to the limitation of extracting any information on the fraction of individual Pd-Ru alloy phase and their structure, with the restriction of EXAFS to distinguish between Ru and Pd atoms due to similar photoelectron scattering amplitude, the single shell fitting was found to be sufficient to fit first FT peak reasonably. Supplementary Figure 2 shows the fitting results of EXAFS for $Pd_{0.5}Ru_{0.5}$ NPs measured at Pd K-edge (left) and Ru *K*-edge (right).

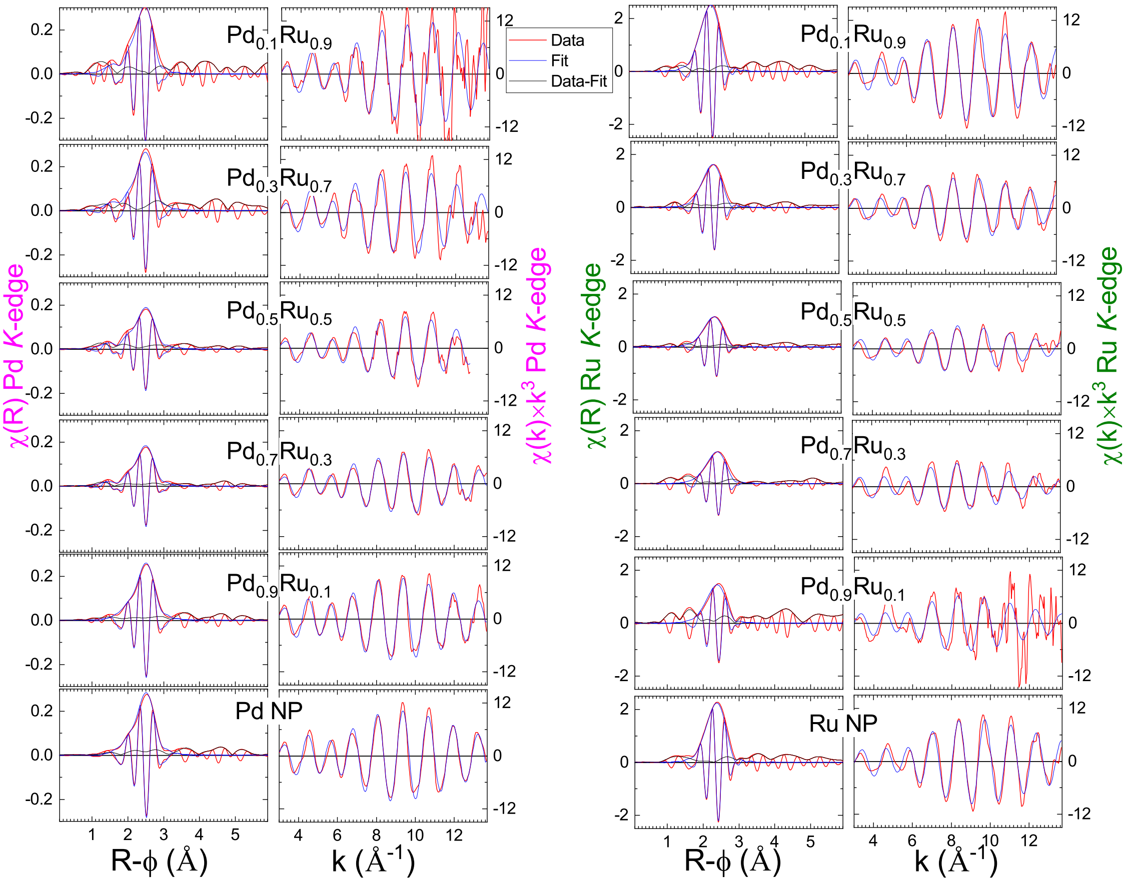

Figure S2. Fitting results of EXAFS

The metrical parameters, obtained from the EXAFS fit shown in Fig. S2, are tabulated in Table S1. Here, R, CN, and σ are first-shell bond distance, coordination number, and root-mean-square displacement, respectively.

Table S1. Metrical parameters obtained from the fitting of EXAFS.

Pd *K*-edge							
	Pd NPs	**Pd$_{0.9}$Ru$_{0.1}$**	**Pd$_{0.7}$Ru$_{0.3}$**	**Pd$_{0.5}$Ru$_{0.5}$**	**Pd$_{0.3}$Ru$_{0.7}$**	**Pd$_{0.1}$Ru$_{0.9}$**	
R	2.72±0.01	2.72±0.01	2.71±0.01	2.70±0.01	2.70±0.01	2.69±0.01	
CN	9.9 ± 1.1	9.7±1.0	6.4±1.2	6.4±1.1	9.0±1.1	8.1±1.0	
σ	0.08±0.01	0.08±0.01	0.08±0.01	0.08±0.01	0.08±0.01	0.07±0.01	
χ^2 error	0.169	0.171	0.114	0.153	0.262	0.405	
Ru *K*-edge							
		Pd$_{0.9}$Ru$_{0.1}$	**Pd$_{0.7}$Ru$_{0.3}$**	**Pd$_{0.5}$Ru$_{0.5}$**	**Pd$_{0.3}$Ru$_{0.7}$**	**Pd$_{0.1}$Ru$_{0.9}$**	**Ru NPs**
R		2.68±0.01	2.67±0.01	2.65±0.01	2.66±0.01	2.67±0.01	2.67±0.01
CN		5.7±1.0	6.1±0.9	4.2±0.9	5.5±0.9	8.5±1.1	7.0±0.9
σ		0.08±0.01	0.09±0.01	0.08±0.01	0.08±0.01	0.08±0.01	0.08±0.01
χ^2 error		3.32	1.107	0.984	1.101	1.71	1.46

SUPPORTING NOTE D. XANES analysis

Supplementary Figure 3 shows XANES profile of the Pd$_x$Ru$_{1-x}$ samples measured at (a) Pd and (b) Ru *K*-edge.

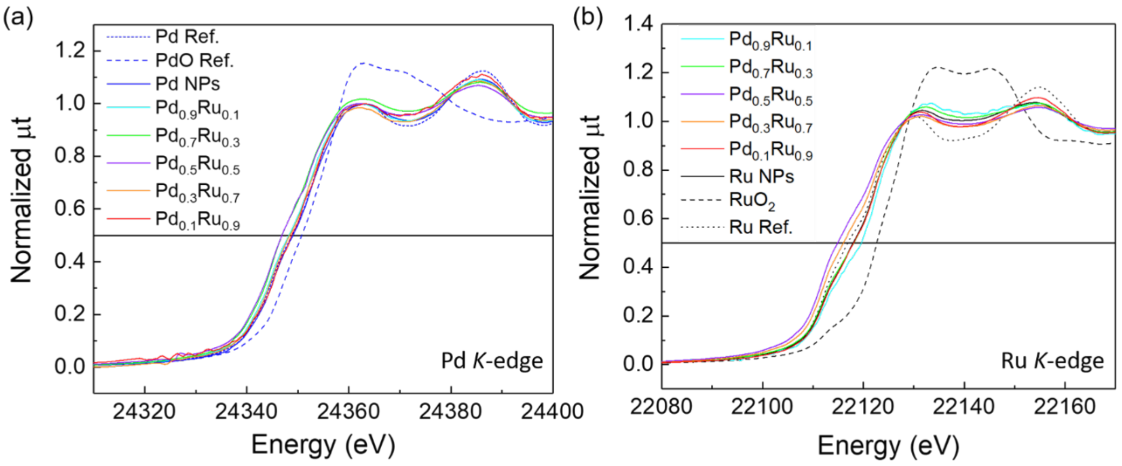

Figure S3. XANES profile of (a) Pd K-edge and (b) Ru K-edge for Pd$_x$Ru$_{1-x}$ NPs and the references.

SUPPORTING NOTE E. VB HAXPES spectra for Ru NPs and Pd NPs

Supplementary Figure 4 shows the VB HAXPES spectra for Ru NPs and Pd NPs. The most apparent difference between Ru NPs and Pd NPs that Pd NPs is more distributed than Ru NPs for a peak intensity in -0.2 ~ 2.0 eV and Ru NPs is more distributed than Pd NPs for a peak intensity in 4.3 ~ 8.0 eV.

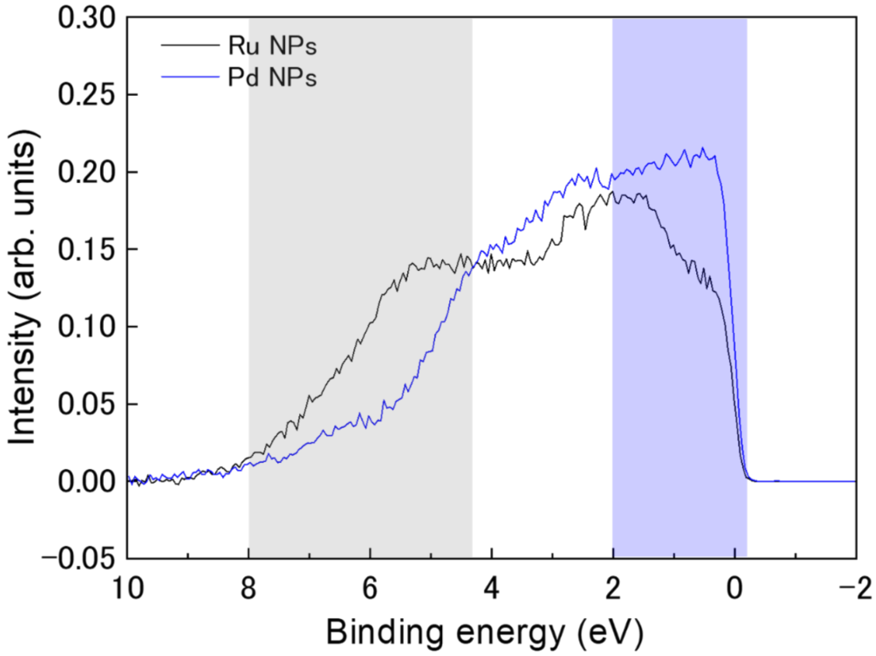

Figure S4. VB HAXPES spectra for Ru NPs and Pd NPs.